Hierarchical structures formed by partially crystalline polymers in solution: from fundamentals to applications – a combined conventional, focusing and ultra-small-angle neutron scattering study

Aurel Radulescu,[a]* Dietmar Schwahn,[a] Jörg Stellbrink,[a] Emmanuel Kentzinger,[a] Lewis J. Fetters[b] and Dieter Richter[a]

[a]Institute for Solid State Research, Research Centre Jülich, 52425 Jülich, Germany, and [b]School of Chemical and Biomolecular Engineering, Cornell University, Ithaca NY, 14853-5021, USA. Correspondence e-mail: a.radulescu@fz-juelich.de

Multilevel aggregates with characteristic sizes covering four orders of magnitude, from 1 nm to 10 µm, are formed upon cooling decane solutions of poly(ethylene-butene) random copolymers (designated as PEB-n, where n is the number of ethyl side branches per 100 backbone C atoms) and wax-containing mixed solutions. The partially crystalline PEB-7.5 copolymers form two distinct morphologies that evolve on a range of length scales. When these polymers are mixed with wax molecules having a crystallization point lower than the polymer aggregation temperature, a hierarchy of morphologies evolves on decreasing the temperature. The multilevel structures were elucidated by combining conventional small-angle neutron scattering, focusing small-angle neutron scattering and ultra-small-angle neutron scattering investigations with microscopy. Contrast-matching analysis of the wax and copolymer components within the common morphologies revealed the wax-crystal modification capacity of the PEB-7.5 copolymers. Since the copolymers limit the growth of wax crystals, they are potential pour-point depressants for the fuel industry.

1. Introduction

Crude oils and middle distillate products such as diesel fuel, kerosene or heating oil undergo a degradation of viscoelastic properties upon cooling below ambient temperature because of the precipitation of the long-chain paraffins (or waxes) in plate-like crystals with sizes of hundreds of micrometres and an overall morphology resembling a 'house of cards' (Ashbaugh *et al.*, 2002). The wax crystals cause a reduction of material fluidity and a loss of filterability leading to technical problems related to the plugging of pumps, pipelines and engine filters. The pour point (PP) – the temperature at which the system gels and becomes mechanically rigid – is about 283 K for a typical untreated crude oil (Claudy *et al.*, 1993) and may vary over a wide temperature range below 273 K in the case of untreated diesel fuels.

In order to circumvent these technical problems 'pour-point depressants' are added. Generally, depressants are copolymers consisting of crystalline and amorphous segments that have the capacity to self-assemble in solution without sedimentation even at temperatures well below 273 K. The wax–copolymer interaction in solution yields complex aggregates whose morphology strongly depends on the precipitation temperatures of both components (Radulescu *et al.*, 2003). A good knowledge of self-assembling behaviour in solution, therefore, is required to assess the ability of copolymers to modify the size and the shape of wax crystals appearing in refined fuels.

Polymeric self-assemblies can assume various morphologies. In some cases hierarchical structures are formed as a consequence of macroaggregation processes. An eloquent example is that of diblock copolymers of polyethylene and poly(ethylene-propylene) (PE-PEP). These molecules spontaneously form thin hairy PE platelets (Richter *et al.*, 1997), which, due to van der Waals interactions, stack to form needle-like macroaggregates several micrometres in length.

In this paper we examine the multilevel structures that form upon cooling in solutions of semicrystalline PEB-7.5 poly(ethylene-butene) random copolymers (where 7.5 represents the number of ethyl side branches per 100 backbone C atoms) and in wax-containing mixed solutions. An investigation of morphologies from nanometre to micrometre size was performed by combining three small-angle neutron scattering (SANS) techniques: conventional pinhole SANS, focusing-mirror SANS (f-SANS) and ultra-SANS double-crystal diffractometry (USANS). The wax-modification properties of the PEB-7.5 copolymers were established by contrast-matched SANS analysis of the individual wax and copolymer components found within the common morphologies formed in wax–copolymer mixed solutions. The large-scale morphologies were also investigated by optical and transmission electron microscopy.

2. Experimental

2.1. Samples

The PEB-7.5 copolymers were synthesized by anionic polymerization of butadiene with random alternation of 1,4- and 1,2-monomers (Morton & Fetters, 1975). Hydrogenation of the vinyl

units led to ethyl side branches on the otherwise linear PE. The ethyl-side-branch content, checked by proton nuclear magnetic resonance, was about 7.5 per 100 C atoms in the main chain. Copolymers with two molecular weights, M_W, were prepared, namely 6 and 30 kg mol^{-1}.

The self-assembling properties were investigated in decane solutions (1% polymer volume fraction) over a large temperature range, between the single coil and the aggregation regime (from 358 to 253 K). The PEB-7.5 wax-crystal modification capacity was checked in common wax–copolymer solutions in decane by mixing the low M_W copolymer with a shorter wax (C_{24}) and the high M_W copolymer with a longer wax (C_{36}). In both situations conventional SANS studies (Radulescu *et al.*, 2004) revealed that the copolymer aggregates at temperatures above the appearance of the wax crystals.

In order to achieve the maximum contrast and to minimize the incoherent background, the solutions were prepared in deuterated decane (d-22). For the wax–copolymer mixed solutions two contrast conditions were used in order to study separately the polymer and wax conformation within the common morphologies: (i) rendering the polymer visible by using fully protonated polymers and matching the deuterated wax molecules with the solvent and (ii) rendering the wax visible by using protonated wax molecules and matching the polymer in deuterated state with the solvent (Radulescu *et al.*, 2004).

2.2. Methods

Three types of SANS methods were used at the FRJ-2 research reactor of the Research Centre Jülich. The conventional SANS measurements were performed on the KWS-2 instrument using a neutron wavelength of $\lambda = 7.2$ Å ($\Delta\lambda/\lambda = 10\%$) and a sample-to-detector distance varying from 2 to 20 m, covering a Q range between 0.002 and 0.14 Å^{-1}, where Q is the modulus of the scattering vector, $4\pi(\sin\theta)/\lambda$, with θ being half the scattering angle. The USANS measurements were performed at the DKD double-crystal diffractometer, which, operating with a neutron wavelength $\lambda = 4.5$ Å, could cover a Q range between 2×10^{-5} and 2×10^{-4} Å^{-1}. High Q resolution is achieved only in the horizontal dimension. Therefore slit corrections have been applied (Schwahn & Yoo, 1986).

In order to bridge the 'Q gap' between the USANS and conventional SANS measurements we used the KWS-3 focusing-mirror SANS instrument (Kentzinger *et al.*, 2004). The design of this instrument is based on a one-to-one image of an entrance aperture on a two-dimensional position-sensitive detector by neutron reflection from a double-focusing toroidal mirror. For small entrance apertures (*i.e.* high Q resolution) f-SANS has considerable intensity advantages over a conventional pinhole SANS (Alefeld *et al.*, 1989). Although this idea is quite old (Henke & DuMond, 1953), its technical realization has been possible only in the last decade, due to the development and production of very high quality soft mirrors for X-ray space telescopes (Aschenbach, 1985). Such mirrors fulfil the requirements needed for the smoothness of f-SANS. The KWS-3 instrument is the only SANS instrument working on this principle. The neutron wavelength $\lambda = 12.7$ Å with a spread of $\Delta\lambda/\lambda = 9\%$ and a typical entrance aperture of 2×2 mm^2 permit SANS studies within a Q range 1×10^{-4} to 1×10^{-3} Å^{-1}. This range can be extended up to 2×10^{-3} Å^{-1} using an off-center detector position.

At the KWS-3 and DKD instruments the multiple scattering effects become very important and dominate for sample thicknesses within the range 0.5–2 mm, typical for a conventional SANS experiment. To minimize the contribution of such effects and to have a reasonable sample transmission (higher than 70%) we varied the sample thickness between 0.2 and 0.5 mm.

The micrometre-scale structures were investigated using a Zeiss Axioplan 2 optical microscope with a Linkam THMS600 temperature stage. Observations were made at room temperature and 263 K. The aggregates formed by the combination of high M_W copolymer with the C_{36} wax were also examined with a CM200 Philips transmission electron microscope (TEM).

3. Results

3.1. Self-assembling of PEB-7.5 random copolymers

Recent conventional SANS studies concluded that the self-assembly of PEB-7.5 copolymer in d-22 forms thin rod-like aggregates (about 100 Å in diameter) with a longitudinally modulated density distribution (Radulescu *et al.*, 2004). The rod length is not accessible by conventional SANS since the observed Q^{-1} power law characteristic of scattering from one-dimensional aggregates extends down to the lowest Q observable. Microscopy observations of the polymer solution at room temperature did reveal the presence of some compact dumbbell-like aggregates with sizes of several micrometres. Thus, in order to explore the micrometre length scale and to elucidate the morphology of this copolymer in solution we extended the structural investigation to a lower Q using the f-SANS instrument.

Fig. 1 presents the scattering intensity in absolute units of 1% low M_W PEB-7.5 in d-22 at two temperatures within the aggregation regime. The data were obtained by combining the KWS2 conventional pinhole SANS (Radulescu *et al.*, 2004) and KWS3 f-SANS instruments to reveal the rich structural features of the polymeric aggregates. At 293 K the scattering profile at high Q follows a $Q^{-5/3}$ behavior, which is indicative of polymer chains in a 'good' solvent. At lower Q, however, the scattering pattern displays significant deviations from the single-coil form factor, which indicates that polymers self-assemble yielding larger-scale aggregates. A broad peak-like feature appears at around $Q^* = 0.025$ Å^{-1}. This feature exposes a correlation length scale of about 250 Å. At lower Q the scattering intensity increases dramatically as a Q^{-4} power law terminating in a Guinier-like regime at very low Q. This observation shows the formation of compact aggregates with sizes within the micrometre range.

In comparison with that at 293 K the scattering pattern at 253 K displays major changes at intermediate and high Q but follows the same profile at low Q. The temperature independence of the low-Q scattering shows that the large-scale aggregates neither grow in size nor number. At intermediate Q the scattering profile follows a clear Q^{-1} power law. At high Q there is a transition at same length scale as the correlation distance in the 293 K data. The Q^{-1} power law is indicative of scattering from rod-like aggregates while the intensity drop at high Q may relate to the lateral profile of the polymer rods. The coincidence of the high-Q length scales at 253 and 293 K implies the correlation peak in controlling the internal morphology of the rod-like aggregates. From a detailed analysis as a function of temperature and polymer concentration (Radulescu *et al.*, 2004) it appears that the correlation distance in the 293 K data is related to the alternation of crystalline and amorphous sequences along the polymer rod.

The conventional SANS and f-SANS studies have established that the low M_W PEB-7.5 random copolymer in solution displays a two-stage growth process yielding two separate morphologies that evolve over a range of length scales: (i) the formation of micrometre-size compact aggregates below 313 K according to the low-Q conventional SANS data (Ashbaugh *et al.*, 2002) – this feature is due to the

crystallization of chains containing long methylene sequences; and (ii) the gradual evolution of density-modulated long one-dimensional aggregates below 293 K.

An indirect visualization of the thin polymeric needles by optical microscopy was possible in a common solution of PEB-7.5 copolymer and wax molecules (C_{24}) whose crystallization temperature is much lower than the temperature at which the polymer rods appear (inset of Fig. 1). The formation of one-dimensional wax objects at 263 K is initiated by the primordial rod-like aggregates, which dictate the overall morphology. Thus, the polymer rods are decorated by the wax and can be indirectly detected *via* microscopy.

3.2. Wax crystallization templated by the PEB-7.5 self-assemblies

When the PEB-7.5 copolymers are mixed with wax molecules having a crystallization temperature lower than the polymer self-assembling temperature, a hierarchical morphology develops on decreasing the temperature. Fig. 2 presents separately the polymer and wax scattering patterns from the mixed solution of low M_W PEB-7.5 copolymer and 4% C_{24} wax at two temperatures within the common aggregation regime (well below the temperature of polymer-rod occurrence). The Q^{-2} power law behavior at intermediate Q and the peak at around $Q^* = 0.025$ Å^{-1} shown at 273 K by both components reveal a co-crystallization of polymer and wax into thin, very large platelets forming a correlated arrangement. The platelets extend laterally (perpendicular to the primordial rods) to several micrometres as proven by the Guinier regime identified at very low Q by the USANS under the wax contrast. At 263 K the scattering patterns of the copolymer and wax differ considerably. The polymer still retains the two-dimensional correlated structure as demonstrated by the Q^{-2} power law behavior at intermediate Q and the correlation peak. The low Q data (Fig. 2, top) measured by f-SANS reveal an additional structure, which is that of the large compact polymer
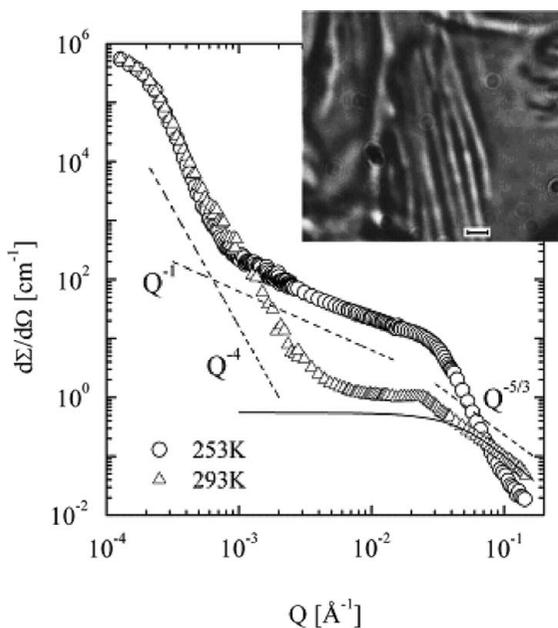
crystals formed at much higher temperatures. A comparison with the case of the polymer self-assembly shows that the addition of wax has only a minor effect on this structural feature.

The wax scattering pattern at 263 K implies that the wax massively crystallizes and grows from thin platelets into large objects with sharp interfaces (Q^{-4} power law at higher Q). The Q^{-2} power law regime identified within the Q range covered by f-SANS proves that these objects are thick platelets. The extra scattering at low Q indicates the formation of additional much larger aggregates whose characterization is difficult due to the absence of sufficient data points in the Guinier range. The one-dimensional morphology tentatively attributed to these aggregates *via* the assignment of the Q^{-1} power law for low Q data is confirmed by the observation of large rods at 263 K (inset of Fig. 1) by optical microscopy.

The wax crystallites appear to decorate the primordial rod-like polymer aggregates. The primordial rods show a longitudinal alternation of crystalline and amorphous sequences. Wax crystallization is apparently mediated by the crystalline parts of this modulated structure. The wax structures grow laterally involving additional polymer chains still in solution. Thus, large common wax–polymer platelets develop around the rods as a secondary morphology. This development explains the change of the scattering behavior from Q^{-1} in the case of wax-free polymer self-assembling to Q^{-2} in the case of co-crystallization of wax molecules in the presence of polymers. The platelets contain most of the material while the primordial rods serve to template the lateral discs in a correlated arrangement resembling a shish kebab. Later crystallization leads to a thickening of the platelets by the wax surplus, which grows from the secondary two-dimensional
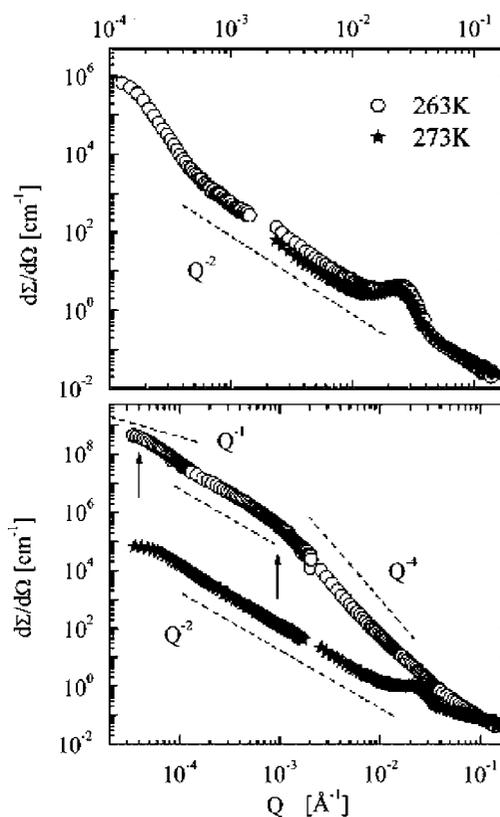

Figure 1
The scattering patterns from a solution of 1% low M_W PEB-7.5 copolymer in d-22 at two temperatures within the aggregation regime. The dotted lines indicate the power law behavior in different Q ranges while the solid line represents the form factor of polymer single coils; the inset shows a micrograph of the aggregates formed in a mixed solution of 0.6% low M_W PEB-7.5 copolymer and C_{24} wax in decane at 263 K (scale bar 10 μm).

Figure 2
Scattering patterns under polymer (top) and wax (bottom) contrast from a mixed solution of 0.6% low M_W PEB-7.5 copolymer and 4% C_{24} wax in d-22 at two temperatures within the common aggregation regime; dotted lines have the same meaning as in Fig. 1; the vertical arrows indicate the observed Guinier regimes within the wax scattering pattern at 263 K.
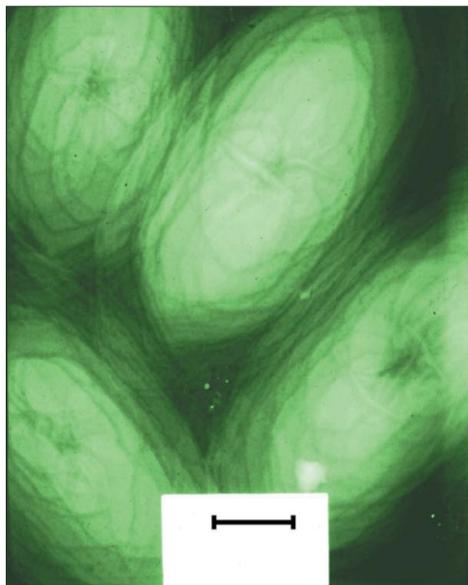
Figure 3
TEM image of the aggregates formed in a decane solution of 1% high M_W PEB-7.5 copolymer and 4% C_{36} wax (scale bar 2 µm).

structures. In this way the correlation effect disappears from the wax scattering pattern and thicker platelets observed at 263 K are formed. These platelets become thicker and join leading to the appearance of a compact one-dimensional tertiary morphology in which the wax encapsulates the primordial rod-like polymer aggregate, as revealed by optical microscopy.

When the high M_W PEB-7.5 copolymer is mixed with C_{36} wax in d-22, almost the same morphological and structural features are observed as in the case of low M_W copolymer and C_{24} wax. The only difference is that the common wax–copolymer correlated platelets occur at much higher temperatures according to the elevated precipitation temperature of both components (Ashbaugh *et al.*, 2002; Radulescu *et al.*, 2004). TEM observations of the common polymer–wax aggregates isolated at room temperature from a decane solution (Fig. 3) reveal stacks of platelets arranged one on top of another and resembling the top view of a shish-kebab-like morphology. The edges of very large platelets and the central axis around which they have irregularly grown are readily visible.

An inspection of the largest structures formed in the mixed wax–copolymer solutions led to the conclusion that clogging of a 45 µm filter – the standard size for defining the 'cold filter plugging point' (CFPP) technical parameter – would not readily occur over a wide range of temperatures in comparison with the undoped wax solutions where very large compact crystals are formed. Thus, the partially crystalline PEB-7.5 copolymer could represent a highly efficient pour-point depressant for middle distillate fuels.

4. Conclusion

By combining SANS techniques covering a wide Q range in reciprocal space with microscopy observations, the morphologies formed in solutions of partially crystalline PEB-7.5 random copolymers and in wax-containing mixed solutions could be resolved. Multilevel structures formed by graded aggregation processes have been identified by a semiquantitative analysis of the scattering patterns. The copolymers form two kinds of aggregates: large compact dumbbell-like objects and rod-like structures with longitudinal modulated density. When these polymers are mixed with waxes having a crystallization point lower than the polymer self-assembling temperature, a hierarchical morphology showing multilevel structures is formed on decreasing the temperature.

References

Alefeld, B., Schwahn, D. & Springer, T. (1989). *Nucl. Instrum. Methods A*, **274**, 210–216.
Aschenbach, B. (1985). *Rep. Prog. Phys.* **48**, 579–629.
Ashbaugh, H. S., Radulescu, A., Prud'homme, R. K., Schwahn, D., Richter, D. & Fetters, L. J. (2002). *Macromolecules*, **35**, 7044–7053.
Claudy, P., Letoffe, J.-M., Bonardi, B., Vassiladis, D. & Damin, B. (1993). *Fuel*, **72**, 821–827.
Henke, B. & DuMond, J. W. M. (1953). *Phys. Rev.* **89**, 1300.
Kentzinger, E., Dohmen, L., Alefeld, B., Rücker, U., Stellbrink, J., Ioffe, A., Richter, D. & Brückel, T. (2004). *Physica B*, **350**, e779–e781.
Morton, M. & Fetters, L. J. (1975). *Rubber Chem. Technol.* **48**, 359–409.
Radulescu, A., Schwahn, D., Monkenbusch, M., Fetters, L. J. & Richter, D. (2004). *J. Polym. Sci. B*, **42**, 3113–3132.
Radulescu, A., Schwahn, D., Richter, D. & Fetters, L. J. (2003). *J. Appl. Cryst.* **36**, 995–999.
Richter, D., Schneiders, D., Monkenbusch, M., Willner, L., Fetters, L. J., Huang, J. S., Lin, M., Mortensen, K. & Farago, B. (1997). *Macromolecules*, **30**, 1053–1069.
Schwahn, D. & Yoo, M. H. (1986). *Springer Proceedings in Physics*, Vol. 10, pp. 83–95. Berlin, Heidelberg, New York, Tokyo: Springer Verlag.